

Facilitated alkali ion transfer at the water  
1,2-dichloroethane interphase: Ab-initio  
calculations concerning alkaline metal cation -  
1,10-phenanthroline complexes.

Cristián G. Sánchez, Ezequiel P. M. Leiva  
Unidad de Matemática y Física,  
Facultad de Ciencias Químicas,  
Universidad Nacional de Córdoba  
Agencia Postal 4, CC 61, 5000 Córdoba, Argentina

Sergio Dassie, Ana M. Baruzzi  
Departamento de Fisicoquímica,  
Facultad de Ciencias químicas,  
Universidad Nacional de Cordoba  
Agencia Postal 4, CC 61, 5000 Córdoba, Argentina

July 6, 2021

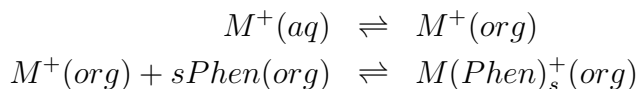
**Abstract**

A series of calculations on the energetics of complexation of alkaline metals with 1,10-phenanthroline are presented. It is an experimental fact that the ordering of the free energy of transfer across the water - 1,2-dichloroethane interphase is governed by the charge / size ratio of the different cations; the larger cations showing the lower free energy of transfer. This ordering of the free energies of transfer is reverted in the presence of 1,10-phenanthroline in the organic phase. We have devised a thermodynamic cycle for the transfer process and by means of ab-initio calculations have drawn the conclusion that in the presence

of phen the free energy of transfer is governed by the stability of the PHEN/M<sup>+</sup> complex, which explains the observed tendency from a theoretical point of view.

## 1 Introduction

Cation transfer across liquid/liquid interphases assisted by complexing agents has been the subject of intensive research in the last years [1, 2, 3, 4, 5]. One main reason is the application of this phenomenon in cation extraction processes [6, 7, 8] and in the development of new ion selective electrodes. In this sense, alkaline and alkaline-earth cations transfer is mainly relevant in the field of clinical chemistry. Many natural and synthetic ligands have been reported [9, 10] and are continuously appearing in an attempt to improve selectivity, increase stability constants of the complex and solubility of the above mentioned ions in the organic phase. Among these compounds, 1,10-phenanthroline is a very well known ligand, especially for transition metals, which are highly soluble in water and have very low selectivity. Alkaline and alkaline-earth cations complexes with 1,10-phenanthroline are also known. Cyclic voltammetry applied to four-electrode systems has been used [11] to analyze the transfer mechanism, nature and stoichiometry of the complexes. The experimental data indicates that in the case of Li<sup>+</sup> the transfer would occur according to the sequence:



where the indices “aq” and “org” indicate aqueous and organic phases respectively and  $s$  denotes the stoichiometry of the metal-phenanthroline complex. In the case where no 1,10-phenanthroline (Phen from now on) is added to the organic phase, the potential of transfer and accordingly the free energy of transfer is lower for larger alkaline cations according to the smaller charge/size ratio for these ions. In the presence of Phen in the organic phase this order in the free energy of transfer is reverted indicating a strong interaction of the ions with smaller radii with Phen.

Synthesis and characterization of 1,10-phenanthroline derivatives have been performed in the last years by different groups [9, 10, 11], the main aim of this research being the development of a Li<sup>+</sup> selective electrode for

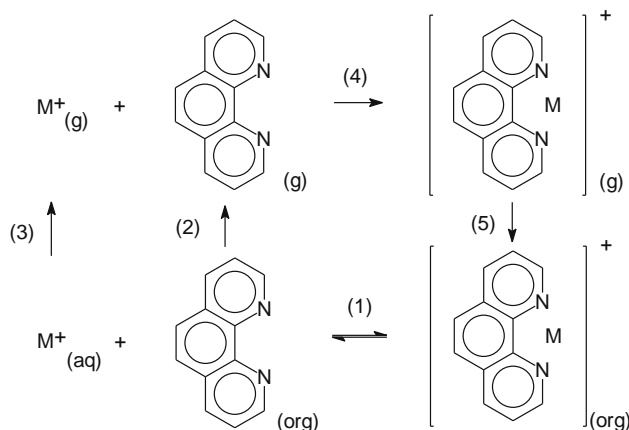


Figure 1: Thermodynamic cycle used to analyze facilitated transfer of alkaline ions assisted by 1,10-phenanthroline.

monitoring  $\text{Li}^+$  activity in biological systems. In this respect, calculation of the interaction energy between ligand and cation would be helpful for the prediction and design of new ionophores.

It is the purpose of the present work to provide a qualitative explanation for some of the above mentioned experimental results concerning the transfer of different alkaline ions through the water/1,2-dichloroethane interphase facilitated by 1,10-phenanthroline.

## 2 The Model

In order to explain the experimental results from a thermodynamic point of view we devised a thermodynamic cycle for the overall transfer process as shown in Figure 1. The global transfer process, here denoted with (1) is divided into a number of elementary steps (2-5) for which we are going to analyze the relative contributions to (1). In step (2) we take phenanthroline, which is dissolved in the organic solvent to the gas phase. We shall denote this contribution with  $-\Delta G^{dis}$ . In step (3) we take an alkaline ion, which is dissolved in the aqueous phase to the vacuum. This step involves a free energy change which is equal to *minus* the solvation free energy of the ion in water  $-\Delta G_{solv}^{M^+}$ . In step (4) we combine the alkaline ion with phenanthroline in the gas phase to yield a compound that we shall denote as  $PhenM^+$ . We label the related free energy change with  $\Delta G_f^{PhenM^+}$ . In step (5) we bring  $PhenM^+$

into the organic phase, with an associated free energy change  $\Delta G_{solv}^{PhenM^+}$ .

In order to consider relative differences between the transfer free energies of the different alkaline ions, we can leave aside the contribution of step (2) (which amounts 68.9 KJ/mol) to the total free energy change, since it is the same for all the ions. If the contribution  $-\Delta G_{solv}^{M^+}$  of step (3) were the dominant one, the overall process would be favored for the bigger ions, as most solvation models state, this desolvation energy is inversely proportional to the radius of the ion. Turning to step (5), the resolution of the complex should involve only a minor contribution to the total free energy, since the charge/size ratio of this species should be almost the same for all the ions. Thus, step (4) must be responsible for the observed trend in the free energy of transfer. In order to check out the validity of this conclusion, we performed a series of ab-initio calculations of the structure of alkaline metal - 1,10-phenanthroline cationic complexes. We analyzed the differences of energy of the complexation process between the different ions in terms of the nature of the chemical bond that is formed.

### 3 Ab-initio calculations

The subject of the present study are the complexes of 1,10-phenanthroline with lithium, sodium and potassium cations ( $Li^+$ ,  $Na^+$ ,  $K^+$ ). The first step of the study was to determine the structure of the different complexes. Geometry optimizations were carried out for 1,10-phenanthroline,  $LiPhen^+$ ,  $NaPhen^+$  and  $KPhen^+$  using STO-3G [15][16][17] and MIDI [18] basis sets at the RHF level, the energies of the single ions  $Li^+$ ,  $Na^+$  and  $K^+$  were also calculated. The results for these energy calculations are shown in Table 1. MP2 corrections  $\Delta E_c$  accounting for the correlation contribution to the total energy were also calculated and added to the RHF/MIDI results, as given in the third column of this table. These corrections include core orbitals and were obtained using the geometries at the energy minimum of the RHF/MIDI results. All calculations were performed at  $C_{2v}$  symmetry.

Table 2 shows the results for the energy change associated with complex formation  $\Delta E_{cf}(PhenM^+)$  at the different levels of theory as calculated from the results from Table 1. In all cases we find the stability of the  $PhenM^+$  complex to increase in the order:  $PhenK^+ < PhenNa^+ < PhenLi^+$ , in agreement with the expectations formulated in the previous section.

Taking into account that the basis sets that were used for the calculation

are small, we must consider that the basis set superposition error (BSSE) associated with the RHF calculation could deliver an important contribution to the energy change of complex formation. The energy differences related to  $\Delta E_{BSSE}$ , defined below, are shown in Table 3 for the RHF calculations with STO-3G and MIDI basis sets, as calculated according to the method of Boys and Bernardi [19]. Within this method, the corrected energy of complex formation  $\Delta E_{cf}^{BSSE-corr}$  is calculated from:

$$\Delta E_{cf}^{BSSE-corr} = E_{cf}(PhenM^+) - E_{Phen}^{M^+-gh} - E_{M^+}^{Phen-gh}$$

where  $E_{PhenM^+}$  is the calculated energy for the complex,  $E_{Phen}^{M^+-gh}$  denotes the energy of Phen when the calculations are performed including the basis functions of  $M^+$  as a "ghost" molecule and  $E_{M^+}^{Phen-gh}$  is the energy of  $M^+$  with the Phen molecule as a ghost. The BSSE is calculated as follows:

$$\Delta E_{BSSE} = \Delta E_{cf}^{BSSE-corr} - \Delta E_{cf}^{uncorr}$$

Since the BSSE error arises from the mathematical fact that the basis sets are not complete, the inclusion of the ghost molecules always produces a lowering of the energy.  $\Delta E_{BSSE}$  is then a positive quantity which will be lower the larger the basis set used for the calculation. Thus,  $\Delta E_{cf}^{uncorr}$  includes some energy that is not related to the chemical reaction itself but with the better description of the wave function of one monomer augmented by the inclusion of the basis set of the other. We find that in the present case  $\Delta E_{BSSE}$  amounts less than 39% and 12% of the binding energy  $\Delta E_{cf}(PhenM^+)$  for the RHF/STO-3G and RHF/MIDI cases respectively.

Another factor to include in the binding energies of  $PhenM^+$  are the corrections for the change in zero point energy (ZPE) between Phen and  $PhenM^+$ . These ZPE values were obtained from a normal mode analysis at the equilibrium geometry at RHF/STO-3G and RHF/MIDI levels of theory, further details about vibrational analysis are given below in section 3. The values for the ZPE correction are given in Table 4. Since upon complex formation new weak bonds are formed, the change in ZPE is always positive and small compared to the total  $\Delta E_{cf}(PhenM^+)$ , amounting less than 1.7 % and 2.4% of the binding energy for the RHF/STO-3G and RHF/MIDI cases respectively.

In Table 5 we show the results for the energy change of complex formation for the different complexes with all corrections included.

Using the theoretical values for the vibrational frequencies, optimized geometries and energy changes calculated ab-initio, we made estimations for the changes in the thermodynamic functions for alkaline metal cation complexation in the gas phase with 1,10-phenanthroline. In Table 6 we show the results for the changes in internal energy, enthalpy, entropy and free energy calculated using normal mode harmonic oscillator, rigid rotor and ideal gas partition functions for the different complexes, metals and Phen. We find that the entropy change is small, arising fundamentally from the loss in translational degrees of freedom upon complexation. Thus, the free energy change of this reaction is energetically dominated at normal laboratory temperatures.

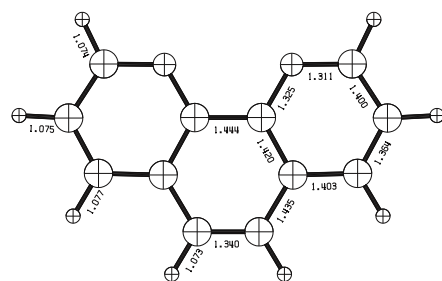
In spite of the fact that the approximations used here make these values only a rough estimation of the real ones, we can clearly see a trend in stability of the different complexes in the order  $\text{Li} > \text{Na} > \text{K}$ . According to the thermodynamic cycle shown in section 1, this would indicate that the free energies of transfer and accordingly the transfer potential for the different ions across the water 1,2-dichloroethane interphase assisted by 1,10-phenanthroline should follow the sequence:

$$\Delta V_K > \Delta V_{Na} > \Delta V_{Li}$$

which is in fact, as we have previously stated, the order found in the voltametric experiment.

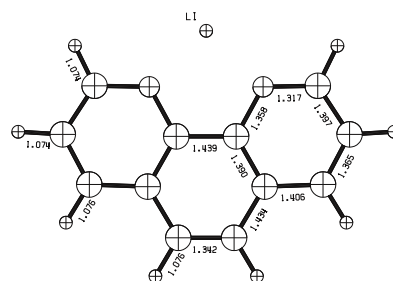
## 4 Structure and vibrational spectra of the complexes

Figure 2 shows the structure of Phen and  $\text{Li}^+$ ,  $\text{Na}^+$  and  $\text{K}^+$  complexes as obtained from RHF/MIDI geometry optimizations. The structure of 1,10-phenanthroline is in very good agreement with reported experimental results based on single crystal X-ray diffraction [20]. The structures of complexes  $\text{PhenLi}^+$  and  $\text{PhenNa}^+$  obtained from the calculations show shorter N-M<sup>+</sup> bond lengths than those obtained from X-ray diffraction experiments [21, 22, 23], this is reasonable since in the crystal there is always a counterion coordinated with the metal cation. Comparison of Phen deformation upon complexation is difficult because in the crystals the Phen molecule is strongly distorted from  $C_{2v}$  symmetry and it is not easy to determine which geometry changes are produced by complexation and which by crystal packing.



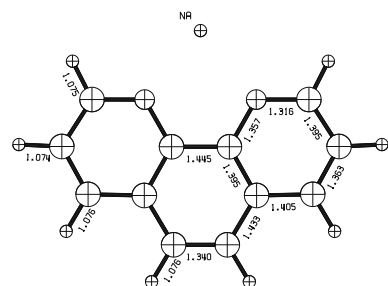
1,10-PHENANTHROLINE RHF/MIDI

(a)



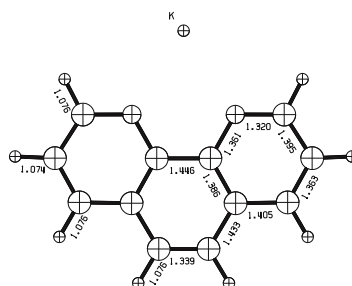
LITHIUM - 1,10-PHENANTHROLINE CATION RHF/MIDI

(b)



SODIUM - 1,10-PHENANTHROLINE CATION RHF/MIDI

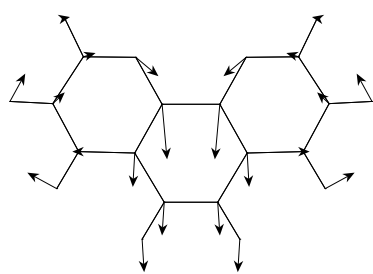
(c)



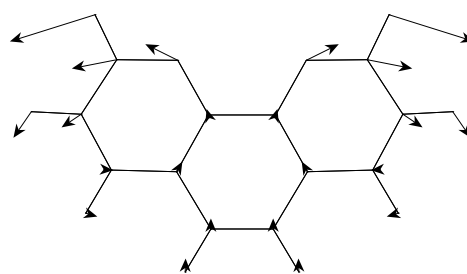
POTASIUM - 1,10-PHENANTHROLINE CATION RHF/MIDI

(d)

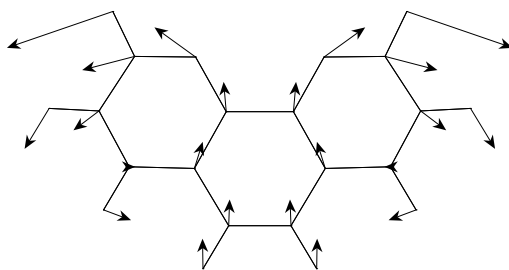
Figure 2: RHF/MIDI structure of Phen and PhenM<sup>+</sup> complexes. All distances are in Å.



(a) 1,10-phenanthroline- $\text{Li}^+$



(b) 1,10-phenanthroline- $\text{Na}^+$



(c) 1,10-phenanthroline- $\text{K}^+$

Figure 3: Perturbation of Phen structure upon complex formation with the different cations.



As we may see at a first glance the major structural difference between the different complexes is the Phen-cation distance, which increases in going from  $\text{Li}^+$  to  $\text{K}^+$  as shown in Table 7, where we report the N- $M^+$  distances  $d_{N-M^+}$  for the different complexes. It is found that  $d_{N-M^+}$  is smaller for  $\text{Li}^+$  and almost the same for  $\text{Na}^+$  and  $\text{K}^+$  complexes.

Figure 3 shows the perturbation of Phen structure produced by the complexation with the different cations. The arrows indicate the direction and relative magnitude of the difference in position between corresponding atoms in the two structures, complexed and free, according to the vector:

$$\Delta \mathbf{r}_i = \mathbf{r}_i^{\text{Phen}M^+} - \mathbf{r}_i^{\text{Phen}}$$

where  $\mathbf{r}_i^{\text{Phen}M^+}$  represents the position vector of atom  $i$  in the complex and  $\mathbf{r}_i^{\text{Phen}}$  the position vector of atom  $i$  in Phen. In order to fix the relative positions between the two molecules for comparison, the coordinates of the different atoms were set so as to minimize the sum of the distances between corresponding atoms,

$$f(\{\mathbf{r}_i\}) = \sum_i \left| \mathbf{r}_i^{\text{Phen}M^+} - \mathbf{r}_i^{\text{Phen}} \right|$$

subject to the constraint of keeping constant the structure of both molecules.

According to this figure we may think of the Phen molecule as a pair of forceps that closes around the ion. The presence of  $\text{Li}^+$  between the forceps originates a closing whereas the presence of  $\text{Na}^+$  or  $\text{K}^+$  originates an opening of the forceps. This observation and the other stated in the previous paragraph may be briefly stated in the following words: complexation occurs when the metal accommodates itself in the "cavity" formed by the two nitrogen atoms in Phen. Since  $\text{Li}^+$  is the smallest, it fits comfortably in this cavity and results in its contraction. On the other hand,  $\text{Na}^+$  and  $\text{K}^+$  are bigger than the size of the cavity, forcing Phen to open for a proper accommodation of the incoming ion.

We turn now to the study of the differences in vibrational spectra between the different complexes involving alkaline ions and Phen. These vibrational spectra were calculated using normal mode analysis at the equilibrium geometry at RHF/MIDI level using force constants calculated from ab-initio analytical second order derivatives of the RHF/MIDI energy. No scaling was done of vibrational frequencies since no predictive analysis is pretended but only a qualitative description of the main changes observed. In figure 4 we

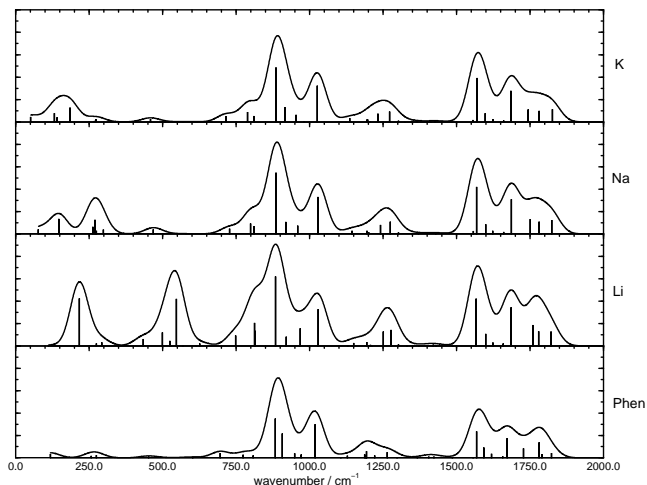


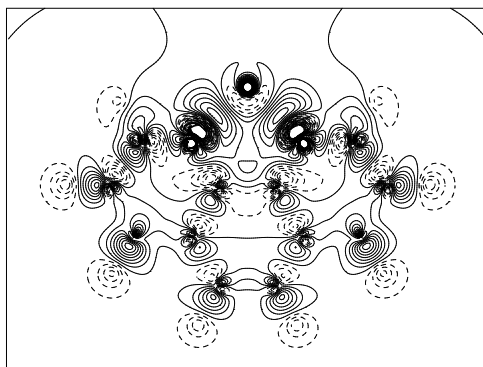
Figure 4: Theoretical non-scaled RHF/MIDI vibrational spectrum of Phen and PhenM<sup>+</sup> complexes. The absorbances are expressed in Debye<sup>2</sup> amu<sup>-2</sup> Å<sup>-2</sup>.

can see the simulated spectra. In order to clarify the main features we have superimposed to the usual line representation a graph obtained by summing gaussian functions centered at each frequency with the corresponding intensity, all of the same amplitude in wavenumber. This construction does not attempt to compare with experimental information but to make easier to detect the main features of the spectra.

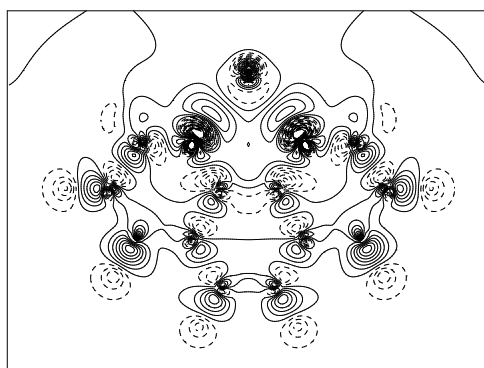
The fundamental differences between the spectra for the different complexes appear mainly in the low frequency bands. Two distinctive bands at 250 cm<sup>-1</sup> and 600 cm<sup>-1</sup> appear in the case of PhenLi<sup>+</sup>, corresponding to Li out of plane bending and Li-Phen stretching respectively. Corresponding bands of PhenNa<sup>+</sup> and PhenK<sup>+</sup> are displaced towards considerably lower frequencies indicating the stronger bonding of Li<sup>+</sup> to Phen with respect to Na<sup>+</sup> and K<sup>+</sup> yielding higher force constants for Li<sup>+</sup>-Phen vibrations.

## 5 Nature of the metal-ligand bond

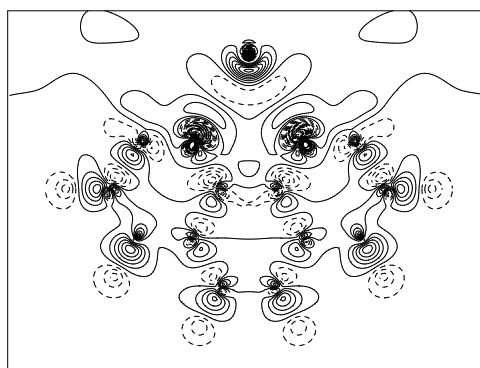
Electronic density difference maps over the  $\sigma_v(xz)$  plane are shown in Figure 5. These maps represent the difference of electronic density between the



(a) 1,10-phenanthroline-Li<sup>+</sup>



(b) 1,10-phenanthroline-Na<sup>+</sup>



(c) 1,10-phenanthroline-K<sup>+</sup>

Figure 5: Electron density difference map upon complex formation for the different complexes. Continuous contour lines indicate positive  $\Delta\rho$  and broken contours indicate negative  $\Delta\rho$ .

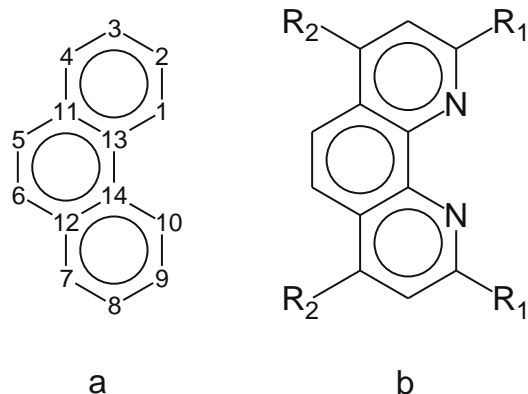


Figure 6: a) numbering scheme used for C atoms, b) Possible positions for selectivity increasing substituents.

complex and the monomers at the equilibrium geometry of the complex:

$$\Delta\rho(x, z) = \rho^{PhenM^+}(x, z) - \rho^{Phen}(x, z) - \rho^{M^+}(x, z)$$

It can be appreciated that the electron withdrawal by the metal ion produces an electron depletion located mainly in the neighborhood of the N lone pair. The increase of positive charge on the N atoms sparks a redistribution of the electronic density via inductive effects across the bonding network. Thus, a concomitant polarization of the C-H bonds occurs in all the molecule. However, this has only a minor effect on the C-H vibrational frequencies and bond distances.

Mulliken analysis of the atomic charge on the different cations is shown in Table 8. The numbering scheme used here for the carbon atoms is shown in Figure 6a. The electronic charge transfer from Phen to the ion seems to be rather small, and almost the same for the three species considered here. According to Mulliken analysis, the carbon atoms which show the largest positive charge accumulation  $\Delta q = q_{complexed} - q_{free}$  are C2, C4 and C13 (and the symmetrical counterparts C9, C7 and C14). In the most relevant case of Li, the sequence found is the sequence  $\Delta q_{C2} > \Delta q_{C13} > \Delta q_{C4}$ . The C2

atom is directly affected by the electron withdrawal at the N atom, remaining its only possibility of recovering electronic charge via inductive effects from C3. On the other hand, C13 accommodates its charge better since it can take charge from two bonds instead of only one. The positive charge of C4 is produced by electron withdrawal through the external and internal bonding network via C11 and C3.

As thoroughly analyzed by Bader[24], the laplacian of the electronic density  $\nabla^2\rho$  can also deliver relevant information concerning the nature of the chemical bond and chemical reactivity. It can be shown that if  $\nabla^2\rho < 0$  at the point  $\mathbf{r}$ , then  $\rho(\mathbf{r})$  is greater than the average of its value over an infinitesimal sphere centered on  $\mathbf{r}$ , while the opposite is true if  $\nabla^2\rho > 0$ . Thus, the laplacian can be used as a criterion for charge concentration or depletion in the different molecular regions, and it defines in the interatomic regions the so called valence-shell charge concentration. This corresponds to the portion of the outer shells of the atoms over which  $\nabla^2\rho < 0$ , that is, the region where the chemically relevant valence electronic charge is concentrated. The contourplot of the laplacian of the electronic density  $\nabla^2\rho$  over  $\sigma_v(xz)$  for the different complexes and Phen are shown in Figure 7 for the region surrounding the N atoms. The analysis of the plots of the laplacian electronic density for the different complexes and Phen shows the bonded charge concentration between the C-N and C-C bonds, as well the non-bonded charge concentration in the neighborhood of the N atoms. Comparison between the plots obtained for a free and for a complexed Phen shows that this molecule is not affected by complex formation even in its finer details and no evidence of a new chemical bond between Phen and the different cations can be found. Furthermore no drastic differences are seen in the plots for the different complexes that cannot be ascribed to the differences in the relative radii of the different cations. Thus, all previously stated observations suggest that the Phen -  $M^+$  bond is mainly of electrostatic nature and that the orders of stability of the different complexes is produced by the differences in ionic radii between the different cations.

## 6 Conclusions

We have used a thermodynamic model to analyze the transfer potential of alkaline ions across water / 1,2-dichloroethane facilitated by 1,10-phenanthroline. Based on ab-initio calculations we have concluded that this process is domi-

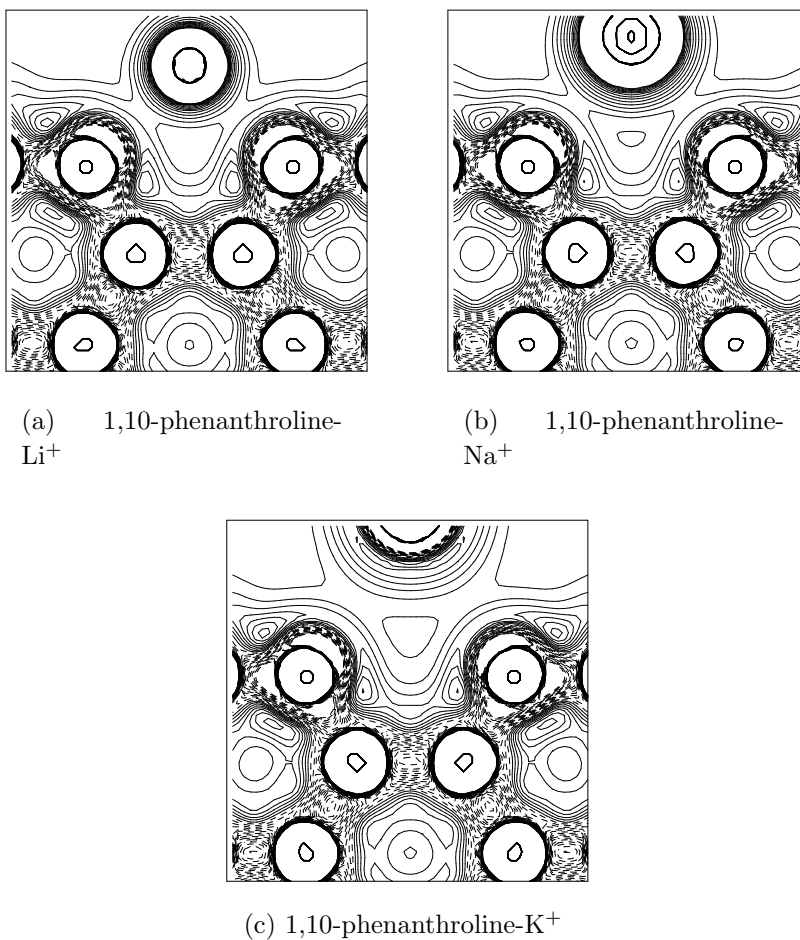


Figure 7: Laplacian of the electronic density for Phen and the different complexes. Solid contour lines indicate positive  $\nabla^2\rho$  and broken contours indicate negative  $\nabla^2\rho$ .

nated by the free energy of complex formation.

The differences in energy and structure of the different complexes can be explained by the different radii of the cations since the Phen -  $M^+$  bond is fundamentally of electrostatic (charge - dipole) nature.

According to Mulliken analysis, the carbon atoms that accommodate most of the positive charge upon complex formation are C2, C13 and C4 (and their symmetrically equivalent positions). According to this, substitution in C2 and C4 with inductive electron donors  $R_2$  and  $R_1$  as shown in Figure 6b would increase the selectivity of Phen towards  $Li^+$ .  $R_1$  should be voluminous so as to prevent the accommodation of the larger cations by steric hindrance increasing  $Li^+$  selectivity. The voluminous part of the substituent should not be located at the C atom vicinal to the ring but rather in the second C atom so as to produce stronger disturbance for Na and K which are located farther than Li in the equilibrium structures. Experimental evidence indicates that 2,9-dibutyl-1,10-phenanthroline shows excellent selectivity coefficients towards  $Li^+$  [13, 25]; substitution at positions 4 and 7 with phenyl rings increases this selectivity but not very strongly. This fact supports our conclusions and leads us to state that it should be possible to predict qualitative tendencies in selectivities of different ligands performing *ab-initio* and probably semiempirical quantum mechanical calculations on the energetics of complexation. This must be done taking into account that, at least for the singly charged cations, the complexation step of the cation plays a dominant role in the energetics of transfer. In the case of doubly charged cations, the solvation energy increases considerably in magnitude (it scales with the square of the charge) and may have a more important contribution to the thermodynamics of the ion transfer. This may explain why 2,9-dibutyl-1,10-phenanthroline is selective towards  $Li^+$  even in the presence of  $Mg^{2+}$ .

## 7 Acknowledgments

All calculations were done in a DIGITAL AlphaStation workstation donated by Alexander von Humboldt Foundation (Germany). A fellowship (C.S.) from the Consejo de Investigaciones Científicas y Técnicas de la Provincia de Córdoba, financial support from the Consejo Nacional de Investigaciones Científicas y Técnicas, the Secretaría de Ciencia y Técnica de la Universidad Nacional de Córdoba and language assistance by Pompeya Falcón are also

gratefully acknowledged.



	RHF/STO-3G	RHF/MIDI	MP2/MIDI*
Phen	-560.982204	-564.572053	-565.813693
LiPhen <sup>+</sup>	-568.346231	-571.901364	-573.135921
NaPhen <sup>+</sup>	-720.808051	-725.382428	-726.620163
KPhen <sup>+</sup>	-1154.095224	-1160.922835	-1162.045787
Li <sup>+</sup>	-7.135447	-7.185210	-7.185210
Na <sup>+</sup>	-159.657383	-160.697965	-160.697965
K <sup>+</sup>	-593.009334	-596.277816	-596.277816

Table 1: RHF energies of Phen, alkaline cations and MPhen<sup>+</sup> complexes at optimized geometries. All values are given in hartrees. \*at RHF/MIDI optimized geometry.

	RHF/STO-3G	RHF/MIDI	MP2/MIDI
$\Delta E_{cf}$ PhenLi <sup>+</sup>	-0.228578	-0.144101	-0.137017
$\Delta E_{cf}$ PhenNa <sup>+</sup>	-0.168462	-0.112410	-0.108504
$\Delta E_{cf}$ PhenK <sup>+</sup>	-0.103685	-0.072965	-0.045723

Table 2: Energies of MPhen<sup>+</sup> complex formation at the different levels of theory. All values are given in hartrees.

	RHF/STO-3G	RHF/MIDI
PhenLi <sup>+</sup>	0.058545	0.005279
PhenNa <sup>+</sup>	0.058744	0.013077
PhenK <sup>+</sup>	0.040848	0.005865

Table 3: Basis set superposition errors in the energy of MPhen<sup>+</sup> complex formation. All values are given in hartrees.

	RHF/STO-3G	RHF/MIDI
LiPhen <sup>+</sup>	0.003932	0.004489
NaPhen <sup>+</sup>	0.002371	0.002738
KPhen <sup>+</sup>	0.001594	0.001706

Table 4: Change in zero point energy upon MPhen<sup>+</sup> complex formation at the different levels of theory. All values are given in hartrees.

	RHF/STO-3G	RHF/MIDI
PhenLi <sup>+</sup>	-0.166101	-0.134333
PhenNa <sup>+</sup>	-0.107347	-0.096594
PhenK <sup>+</sup>	-0.061242	-0.065393

Table 5: Energy change upon MPhen<sup>+</sup> complex formation. These values include BSSE and ZPE corrections. All values are given in hartrees.

Ion	$\Delta U/kJ mol^{-1}$	$\Delta H/kJ mol^{-1}$	$\Delta S/J mol^{-1}K^{-1}$	$\Delta G/kJ mol^{-1}$
Li <sup>+</sup>	-354.38	-356.86	-121.43	-320.66
Na <sup>+</sup>	-253.41	-255.89	-118.10	-220.68
K <sup>+</sup>	-170.24	-172.71	-108.07	-140.49

Table 6: Theoretical values for the thermodynamic functions of reaction of an alkaline ion  $M^+$  with a phenanthroline molecule  $Phen$  in the gas phase to give  $M(Phen)^+$  at 298K, using RHF/MIDI geometries and vibrational frequencies.

	N-M <sup>+</sup> distance
LiPhen <sup>+</sup>	1.921
NaPhen <sup>+</sup>	2.218
KPhen <sup>+</sup>	2.264

Table 7: N-M<sup>+</sup> distances in the different complexes in Å.

	$q_{M^+}^{Mull}$
LiPhen <sup>+</sup>	0.93
NaPhen <sup>+</sup>	0.94
KPhen <sup>+</sup>	0.96

Table 8: Cation charge  $q_{M^+}^{Mull}$  according to Mulliken atomic populations over M in the different complexes.

## References

- [1] P.D. Beattie, R.G. Wellington, H.H. Girault, *J. Electroanal. Chem.* 396 (1995) 317.
- [2] M. Senda, T. Kakiuchi, T. Osakai, *Electrochim. Acta* 36 (1991) 253.
- [3] Y. Kudo, Y. Takeda, H. Matsuda, *J. Electroanal. Chem.* 396 (1995) 333.
- [4] Z. Hu, W. Zhang, P. Zhao, D. Qi, *Electroanalysis* 7 (1995) 681.
- [5] L.M. Yudi, A.M. Baruzzi, V.M. Solis, *J. Electroanal. Chem.* 328 (1992) 153.
- [6] R. A. Sachleben, B.A. Moyer, *J. Driver, Sep. Sci. Technol.* 30 (1995) 1157.
- [7] T. Sasaki, S. Umetani, Q.T.H. Le, M. Matsui, S. Tsurubou, *Analyst* 121 (1996)1051.
- [8] Y. Deng, R.A. Sachleben, B.A. Moyer, *J. Chem. Soc. Faraday Trans.* 91 (1995) 4215.
- [9] D. Lee, J.D.R. Thomas, *Talanta* 41 (1994) 901.
- [10] H. Sugihara, J. Kajiwara, S. Akabori, K. Hiratani, *Chem. Lett.* 1 (1996) 15.
- [11] S.A. Dassie, L.M. Yudi, A.M. Baruzzi, *Electrochim. Acta* 40 (1995) 2953.
- [12] L.X. Sun, T. Okada, J.P. Collin, H. Sugihara, *Analytica Chimica Acta*, 329 (1996) 57.
- [13] H. Sugihara, T. Okada, K. Hiratani, *Anal. Sci.* 9 (1993) 593.
- [14] M. W. Schmidt, K. K. Baldrige, J. A. Boatz, S. T. Elbert, M. S. Gordon, J. H. Jensen, S. Koseki, N. Matsunaga, K. A. Nguyen, S. J. Su, T. L. Windus, M. Dupuis. *J. A. Montgomery, J. Comput Chem*, 14 (1993), 1347.

- [15] W. J. Hehre, R. F. Stewart, J. A. Pople, *J. Chem. Phys.* 51 (1969), 2657.
- [16] W. H. Hehre, R. Ditchfield, R. F. Stewart, J. A. Pople, *J. Chem. Phys.* 52 (1970), 2769.
- [17] M. S. Gordon, M. D. BJORKE, F. J. Marsh, M. S. Korth, *J. Am. Chem. Soc.* 100 (1978), 2670.
- [18] S. Huzinaga, J. Andzelm, M. Klobukowski, E. Radzio-Andzelm, Y. Sakai, H. Tatewaki, "Gaussian Basis Sets for Molecular Calculations", Elsevier, Amsterdam, 1984.
- [19] S. F. Boys, F. Bernardi, *Mol. Phys.* 19 (1976) 325.
- [20] S. Nishigaki, H. Yoshioka, K. Nakatsu, *Acta Cryst.*, B 34, (1978) 875.
- [21] M. Hundal, G. Sood, P. Kapoor, N. Poonia, *J. Cryst. Spec. Research*, 21 (1991) 395.
- [22] M. Hundal, G. Sood, P. Kapoor, N. Poonia, Tiekink, *J. Cryst. Spec. Research*, 22 (1992) 629.
- [23] D. Hughes, *J. C. S. Dalton*, 421 (1973) 2347.
- [24] F. W. Bader in *Atoms in Molecules, A Quantum Theory*. Chapter 7. Oxford University Press, New York (1990)
- [25] H. Sugihara, J. Collin, K. Hiratani, *Chem. Lett. Chem. Soc. Jap.* (1994) 397.